Supporting Information for "Molecular Engineering of Fluoroether Electrolytes for Lithium Metal Batteries"

Yuxi Chen[1], Elizabeth M.Y. Lee[1], Phwey S. Gil[1], Peiyuan Ma[1], Chibueze V. Amanchukwu[1,*], Juan J. de Pablo[1,2,*]

[1]Pritzker School of Molecular Engineering, University of Chicago, Chicago, IL, USA

[2]Center for Molecular Engineering, Argonne National Laboratory, Lemont, IL, USA

CONTENTS

S.1. CHARGE RE-SCALING FACTORS

As discussed in the main text, we applied a charge rescaling factor of 0.8 to correct for lack of considerations of charge transfer phenomenons in ion pairs of non-polarizable forcefields, such as OPLS-AA.[1] With this charge rescaling factor, we managed to get both dynamical properties and conformational properties of our systems to match with experimental measurements. Just to get a more complete picture on the effect of charge rescaling on the solvent systems we studied, we also carried out simulations a charge rescaling factor of 0.7[2,3] and with no charge rescaling at all. The resulting dynamical properties and conformational properties of each studied systems are depicted in Figure S.1. When using a charge rescaling factor of 0.7, we can see that the Li^+ diffusivity matched well with experimental measurements at 300K but we do not see any lithium ion aggregate in E3F1 or E3F2, as we observed in experimental measurements, thus indicating a significant deviation from the reality. Meanwhile, when using no charge rescaling at all, we did see a fraction of lithium ion aggregates in E3F1 and E3F2 as we did in experiments, but the calculated Li^+ diffusivities are more than an order of magnitude different from experimental measurements, indicating an inaccurate representation of the solvent dynamic properties.The predicted diffusivity using the scaling factor of 0.8 shows reasonable agreement with experimental measurements, with differences less than a factor of two. Additionally, using a factor of 0.8 accurately characterized the ion aggregates in E3F1 and E3F2 as observed in the experiments. Thus, all our results from MD simulations reported in the main text are carried out using this charge rescaling factor of 0.8.

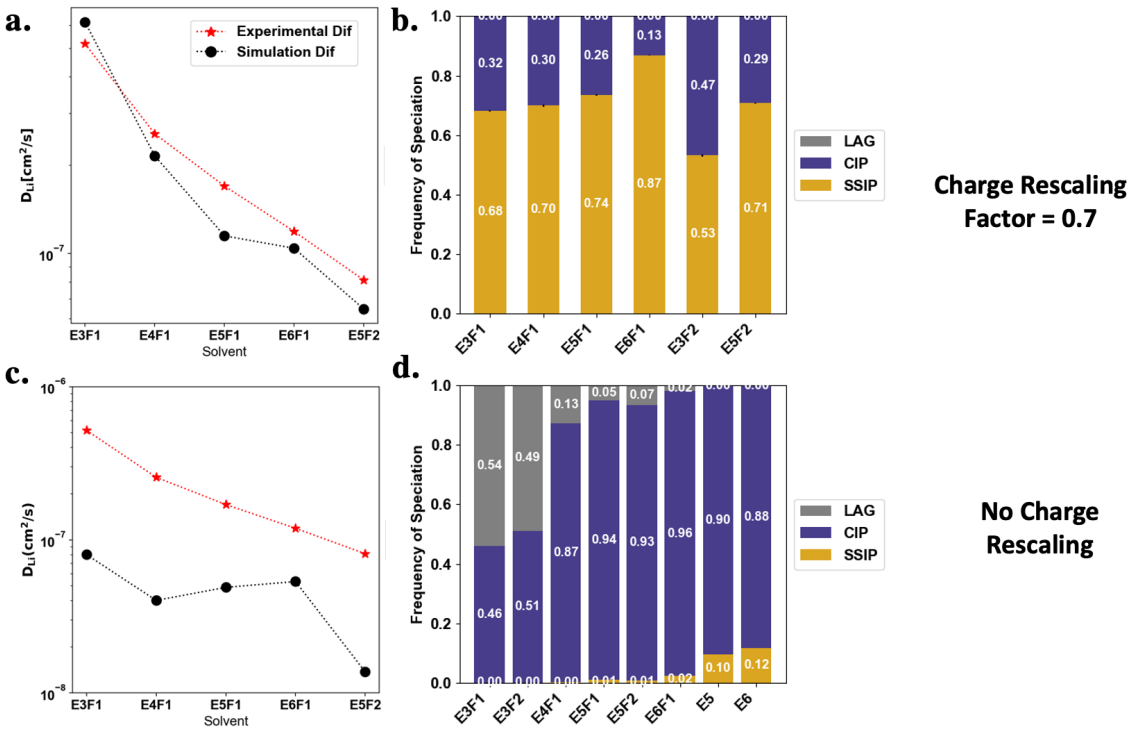

FIG. S.1. Comparison between calculated Li-ion diffusivity from simulation (plotted in black) at 300 K and measured Li-ion diffusivity from experiments (plotted in red) at 300 K, and frequency of Lithium-ion aggregate, Contact ion pairs, and Solvent separated ion pairs in each of solvent systems at 300 K for (a) using a charge rescaling factor of 0.7 and (b) using no charge rescaling at all.

S.2. SOLVENT DENSITIES

The densities of each solvent systems, without addition of salts, were calculated at 300K and compared to experimental measurements at the same temperature. The errors between simulation and experiments are shown in Table S.2

Solvent	**Simulation**	**Experiment**	**% Error**
E3F1	1.26	1.28	1.6%
E4F1	1.25	1.25	0.0%
E5F1	1.24	1.24	0.0%
E6F1	1.22	1.21	0.9%
E3F2	1.38	1.37	0.7%
E5F2	1.33	1.31	1.5%

TABLE S.1. Comparison between simulation calculated densities and experimental measurements

S.3. SIMULATION DETAILS

All molecular dynamic simulations were carried out in a cubic box with the specifications shown in Table S.2:

Solvent	**Number of Solvent Molecules**	**Number of Li^+ Ions**	**Simulation Box Length(nm)***
E3F1	350	75	5.10
E4F1	400	100	5.64
E5F1	350	101	5.65
E6F1	300	99	5.60
E3F2	350	94	5.52
E5F2	350	120	5.99

*:Simulation box length measured at 300K at a concentration of 1M salt.

TABLE S.2. Details on simulation setup on each electrolyte systems.

S.4. ANION DIFFUSIVITY DATA AND TRANSFERENCE NUMBER

The temperature dependent diffusivities of the anion, FSA^-, are shown in S.2. We estimated the transference number from the diffusivity data, defined as $t_+ = D_{Li^+}/(D_{Li^+} + D_{FSA^-})$. The results are plotted in S.2. The calculated transference numbers are also consistent with experimental results.[?]

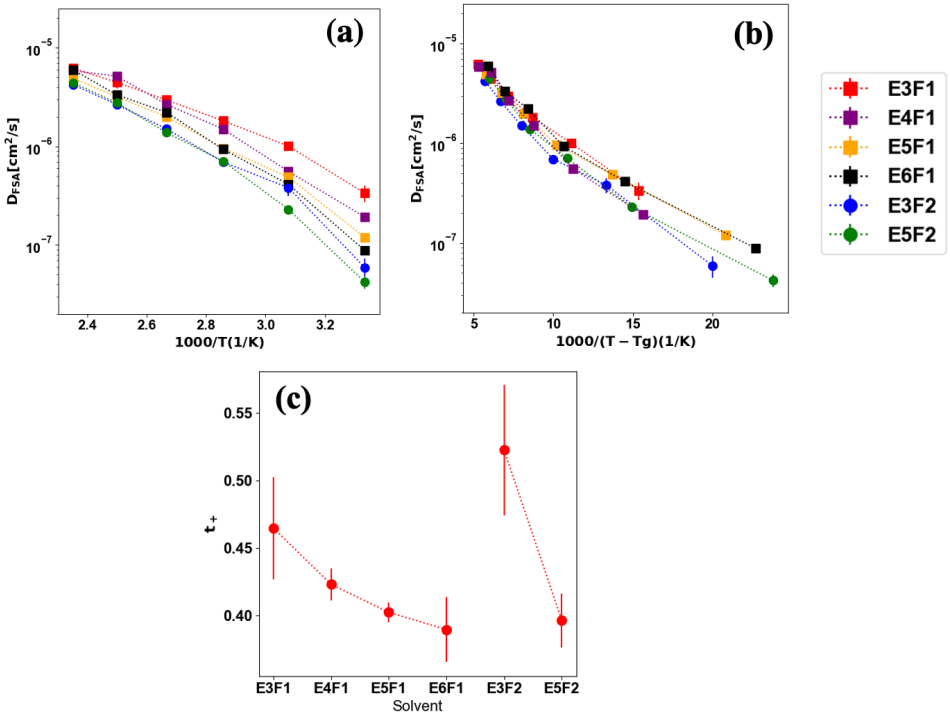

FIG. S.2. Temperature dependent behavior of FSA anion diffusion and Lithium transference number in different systems at 300K. (a)FSA anion diffusivity (D_{FSA^-}) in 1M LiFSA plotted against the scaled inverse temperature, 1000/T, where T is the absolute temperature. (b) Same data as in (a) plotted against scaled reduced temperatures, $1000/(T - T_g)$, where T_g is the glass transition temperature for pure solvents. (c) Lithium transference number for each solvent systems at 300K. Each data point is an average over three independent MD simulations with an error bar for the standard deviation.

S.5. RADIAL DISTRIBUTION FUNCTIONS

The radial distribution functions (RDF) between Li^+ ions and oxygen atoms from the solvents and between Li^+ ions and fluorine atoms from the solvents were calculated respectively, shown in Figure S.3 We can see that Li^+ ions mostly coordinate with oxygen atoms but not with fluorine atoms. Based on the RDF between Li-ion and oxygen atoms, we defined the first solvation shell of Li-ion to be within 0.27 nm, where the first peak ends.

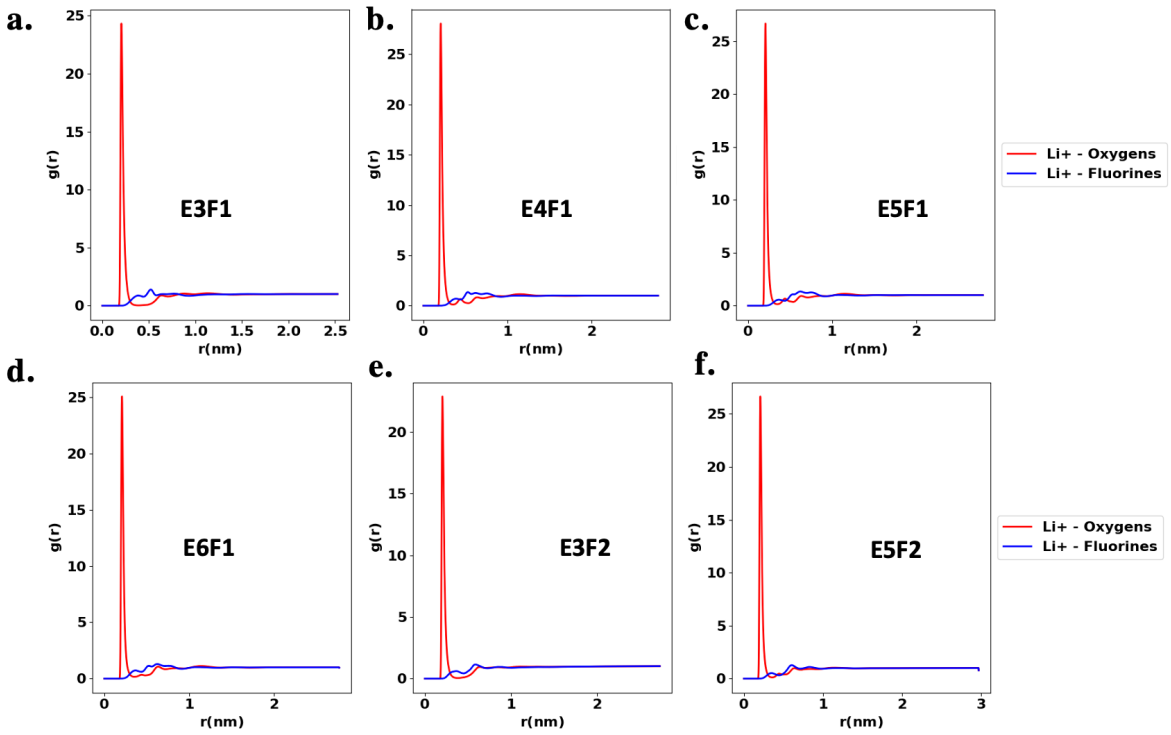

FIG. S.3. RDFs between Li^+ ions and oxygen atoms and between Li^+ ions and fluorine atoms in 1M solvent systems of (a) E3F1 (b) E4F1 (c) E5F1 (d) E6F1 (e) E3F2 (f) E5F2

We further calculated the RDFs between Li^+ ions and oxygen atoms of different proximity to fluorinated terminal groups in the solvent chain, as shown in Figure S.4. The data show that the further the oxygen atom is to the fluorinated terminal group, the more it coordinates with Li^+ ions. The bulk fluorinated terminal group potentially block the Li^+ ions from approaching and coordinating with nearby oxygen atoms.

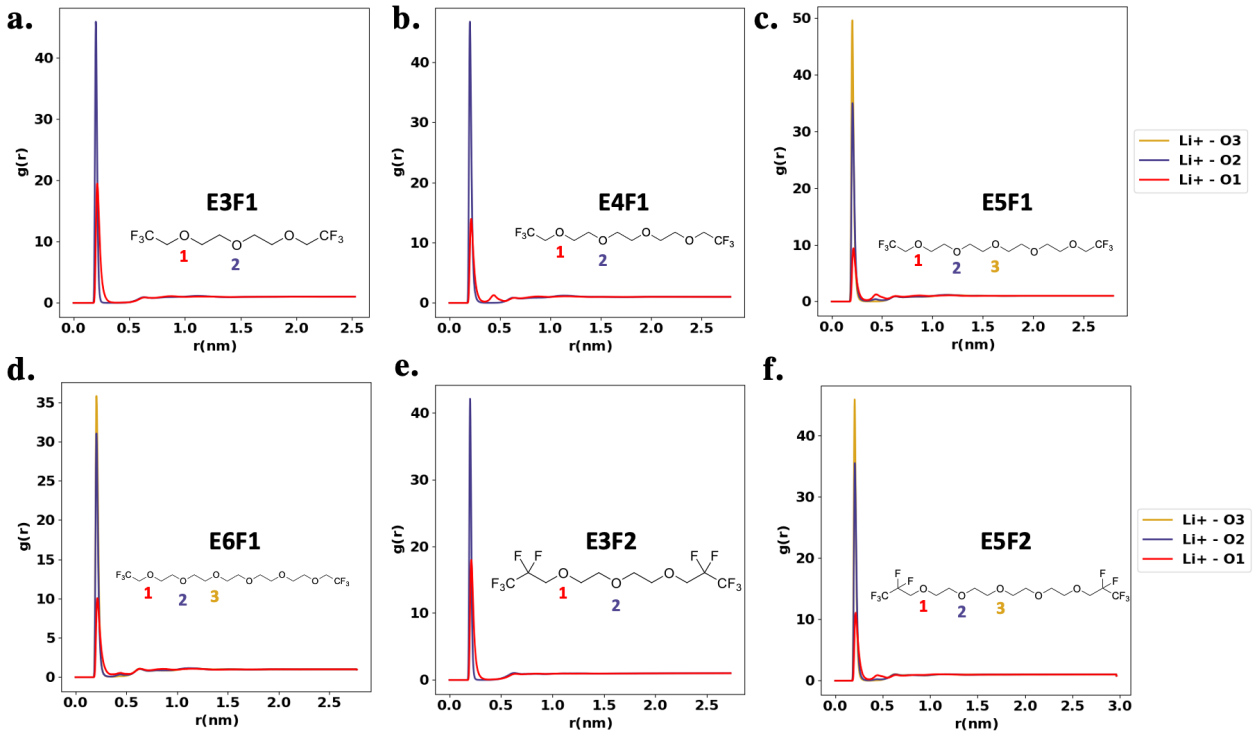

FIG. S.4. RDFs between Li^+ ions and oxygen atoms with different proximity to fluorinated terminal groups in the solvent chain in 1M solvent systems of (a) E3F1 (b) E4F1 (c) E5F1 (d) E6F1 (e) E3F2 (f) E5F2. The oxygen atoms were numbered such that O1 is the closest to the fluorinated terminal group, O2 is the next closest, and etc..

S.6. LITHIUM-ION HOPPING STUDY

The ion-hopping events of lithium-ion relative to the solvent chains were evaluate by calculating the correlation function CACF:

$$CACF(t) = \frac{|S(t+t_0)| \cap |S(t_0)|}{|S(t_0)|} \tag{S.1}$$

Here, $|S(t_0)|$ is the set of ether oxygen atoms from the solvent chain that are coordinating with the lithium-ion at time t_0, and $|S(t+t_0)|$ is the set of ether oxygen atoms coordinating with the lithium-ion at time $t+t_0$. The correlation function CACF was calculated by averaging over all lithium-ions in the system. The correlation function quantitatively characterizes the time needed for a lithium-ion to unbind with a solvent chain and helps us understand the difference in in hopping rate in each of the electrolyte systems studied. The faster the correlation function decays, the more frequent ion-hopping events take place in electrolyte systems. The CACF was calculated at 425K in 1M systems. We used an elevated temperature to accelerate ion dynamics. We used a 50 ns trajectory to calculate the correlation function and moving average was taken to an interval of up to 40 ns. The data is shown in S.5.

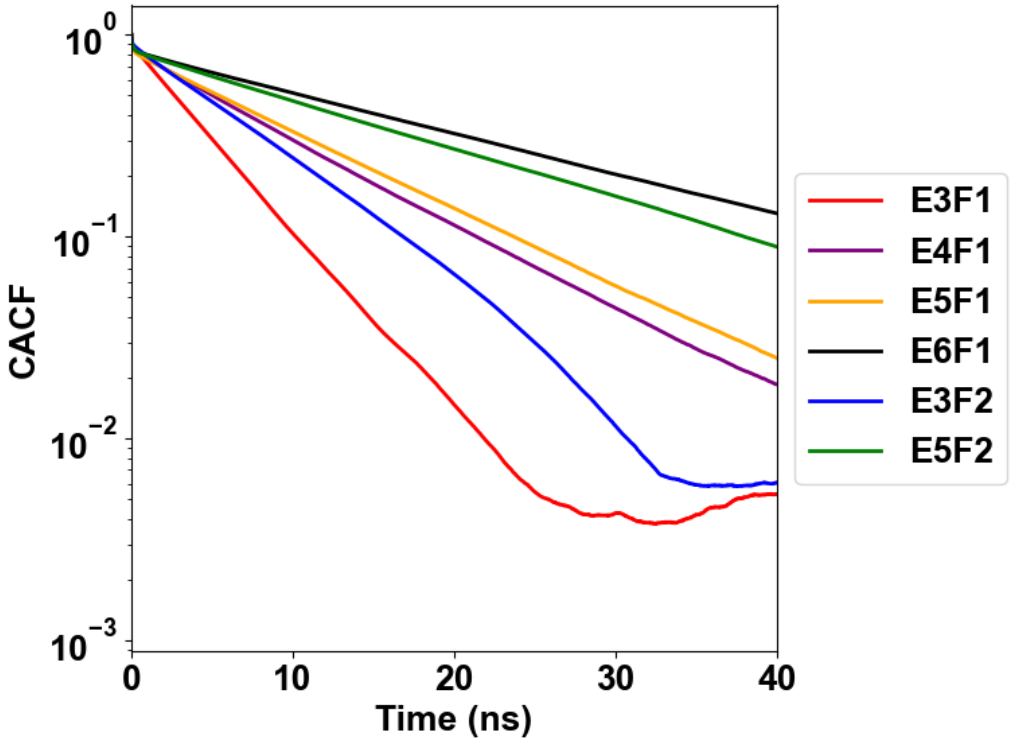

FIG. S.5. Ion hopping correlation function at 425K in 1M electrolyte systems plotted in a log-log scale.

As mentioned in the main text, the ion-hopping rate is a lot faster in E3F1 and E3F2 than in any of the longer solvent chain systems. Furthermore, we noticed that ion-hopping rate increases with decreasing chain length.

S.7. BINDING MOTIFS

The top two most commonly observed binding conformations of E4F1, E5F2, and E6F1 are shown in Figure S.6.

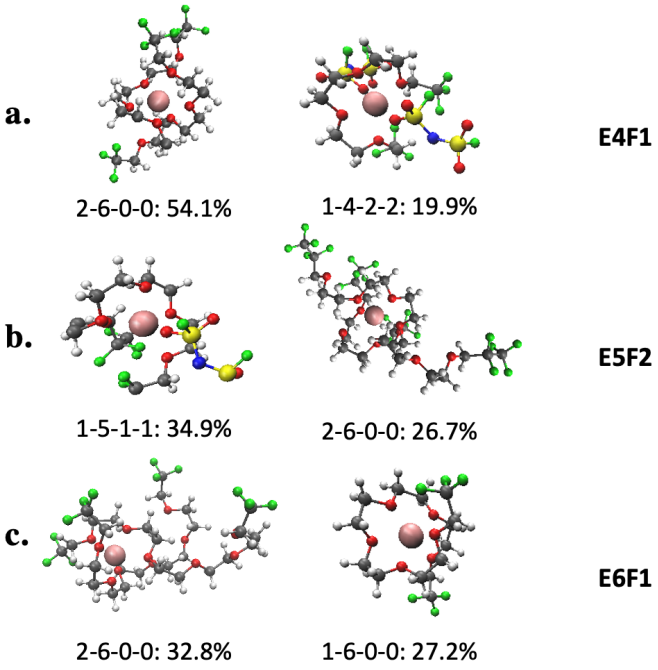

FIG. S.6. Snapshots of the most frequent binding motifs of Li-ion in selected solvent system (E4F1, E5F2, E6F1). The binding motifs are labeled with a 4-digit number, A-B-C-D, where A represents the number of solvent molecules coordinating with Li-ion within the first solvation shell, B represents the total number of ether oxygen from solvent molecules coordinating with Li-ion within the first solvation shell, C represents the number of anion molecules coordinating with Li-ion within the first solvation shell, and D represents the number of oxygens from the anions coordinating with Li-ion within the first solvation shell.

S.8. DIHEDRAL FORCEFIELD

The dihedral parameters of O-C-C-F do not exist in the original OPLS development[4] or the fluorinated alkane extension[5]. Therefore we used the dihedral parameters for O-C-C-H as surrogates due to the similarity of the two dihedrals. To verify the validity of our approximation, we calculated the dihedral potential energy surfaces of ether molecules for both O-C-C-H, and O-C-C-F following the same method described in Jorgensen et al.[4] Dihedral potential energy surfaces were computed using an electronic structure software suite ORCA ver. 5.0.2.[6] Calculations were carried at two different levels: Hartree-Fock, same as in Jorgensen et al.[4] and Density Functional Theory (DFT), using the B3LYP exchange-correlational functional[7]. All calculations used the standard aug-cc-pVTZ basis. At each dihedral angle, geometry was optimized while the dihedral angle, O-C-C-X, was constrained for each ether molecule, CH_4-O-CH_2-CX_3, where X=H or X=F. In Figure S.7, the potential energy surface for the dihedral angles, O-C-C-H and O-C-C-F is shown, one computed at the Hartree-Fock level (Fig. S.7a), while the other at the DFT-B3LYP level (Fig. S.7b). Relative energy is defined as the energy with respect to the global minimum. In both cases, the potential energy difference between X=H and X=F at the maxima is about 3 kJ/mol using Hartree-Fock and 2.5 kJ/mol using DFT-B3LYP. These values are less than $2k_BT$ at $T = 300$ K, the temperature at which all our classical MD simulations are performed. Therefore, dihedral energy langscapes for X=H and X=F appear to be comparable within thermal energy, justifying the use of parameters for O-C-C-H as surrogates to that of O-C-C-F to perform MD simulations.

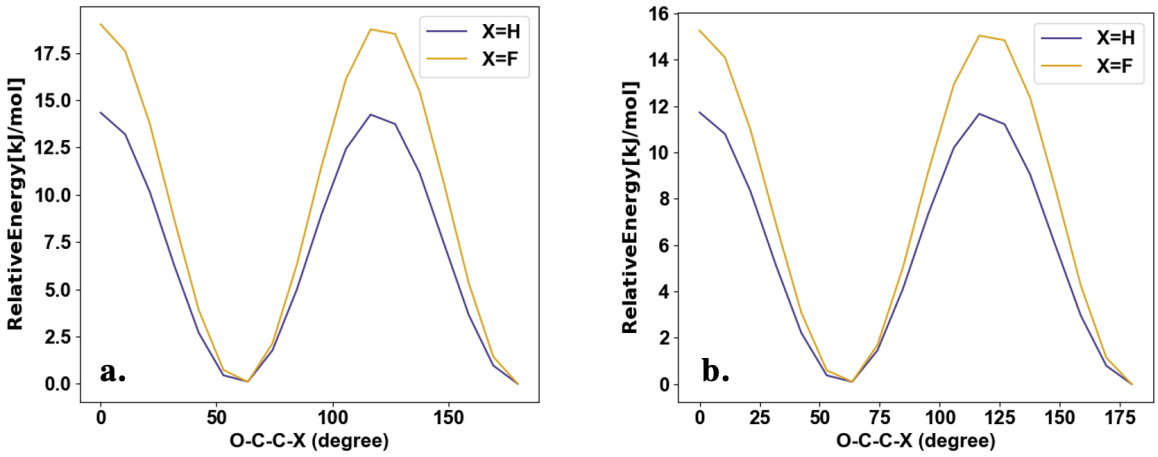

FIG. S.7. Relative potential energy surface comparison between O-C-C-H dihedral and O-C-C-F dihedral in ether molecules, CH_4-O-CH_2-CX_3 where X=H and X=F, calculated using (a) Hartree-Fock and (b)DFT-B3LYP.

S.9. GLASS TRANSITION TEMPERATURE CALCULATIONS

The glass transition temperature of pure solvent systems and 1M solvent systems were calculated by fitting the data of specific volume vs. temperature using first order polynomials as shown in Figure S.8 and S.9 for pure solvents and 1M electrolytes. The intersection of two linear lines is the glass transition temperature for the system of interest[8].The linear regions were determined by the linear fittings that gave a coefficient of determinant R^2 above 0.97. The cooling rate used is 14.2K/ns and temperature range is from 475K to 50K.

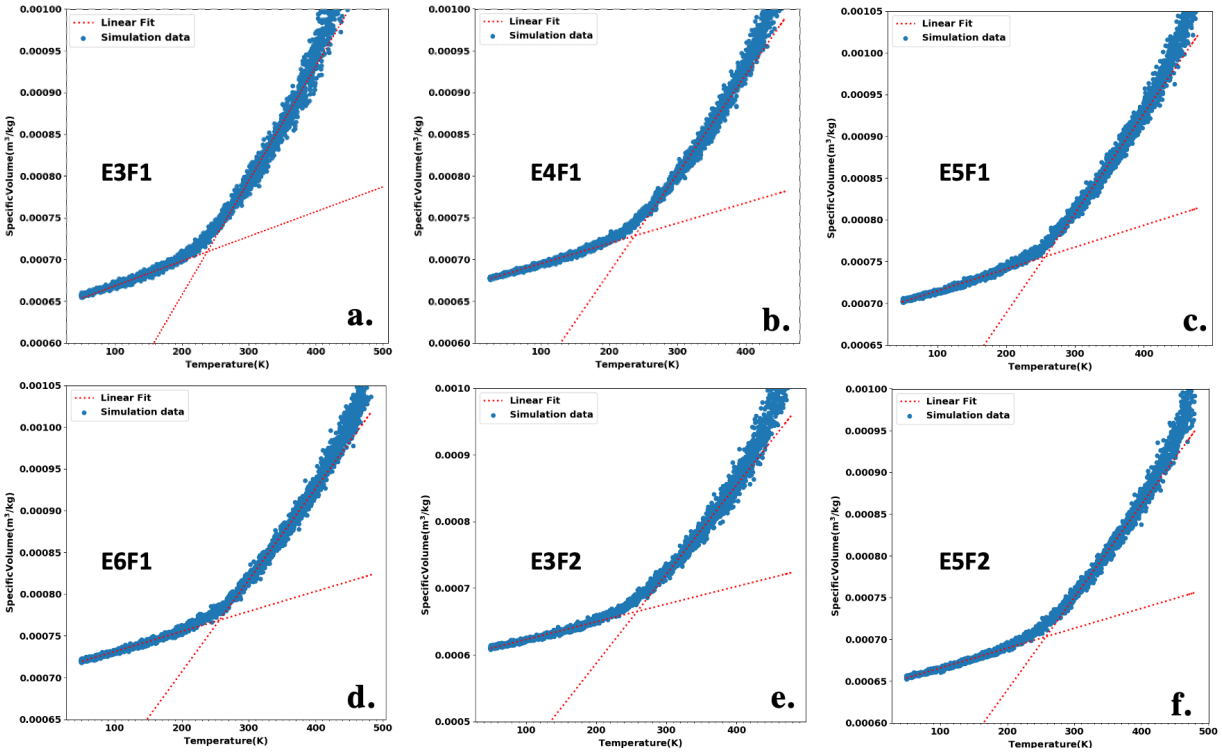

FIG. S.8. Specific volume vs. Temperature plot and linear fitting in pure solvent systems of (a) E3F1 (b) E4F1 (c) E5F1 (d) E6F1 (e) E3F2 (f) E5F2. Simulation data are plotted in blue and the linear fittings are plotted in red dashed lines. The glass transition temperature is the intersection of the two linear lines.

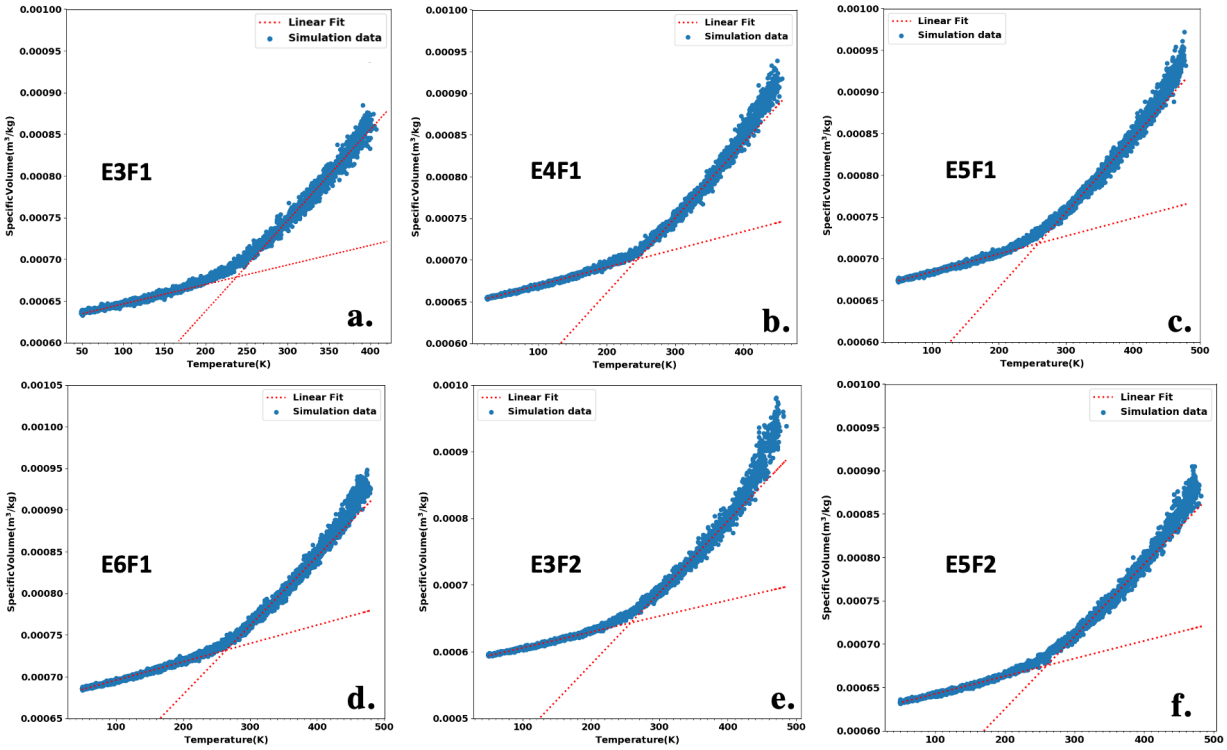

FIG. S.9. Specific volume vs. Temperature plot and linear fitting in 1M solvent systems of (a) E3F1 (b) E4F1 (c) E5F1 (d) E6F1 (e) E3F2 (f) E5F2. Simulation data are plotted in blue and the linear fittings are plotted in red dashed lines. The glass transition temperature is the intersection of the two linear lines.

S.10. MEAN SQUARED DISPLACEMENT PLOTS

The diffusivities were calculated from taking the slope of the Mean Square Displacement(MSD) plots. When calculating the MSDs, moving averages were taken in a 100 ns trajectory in an NVT ensemble in equilibrium. The MSD plots of Li^+ ions at different temperatures in each 1M solvent systems are shown in Figure S.10. The reference line with unity slop was plotted in black dashed lines. We can see that all systems have entered diffusive regime (i.e. had a unity slope) within the 100 ns trajectory, confirming the validity of the calculated diffusivities.[9,10]

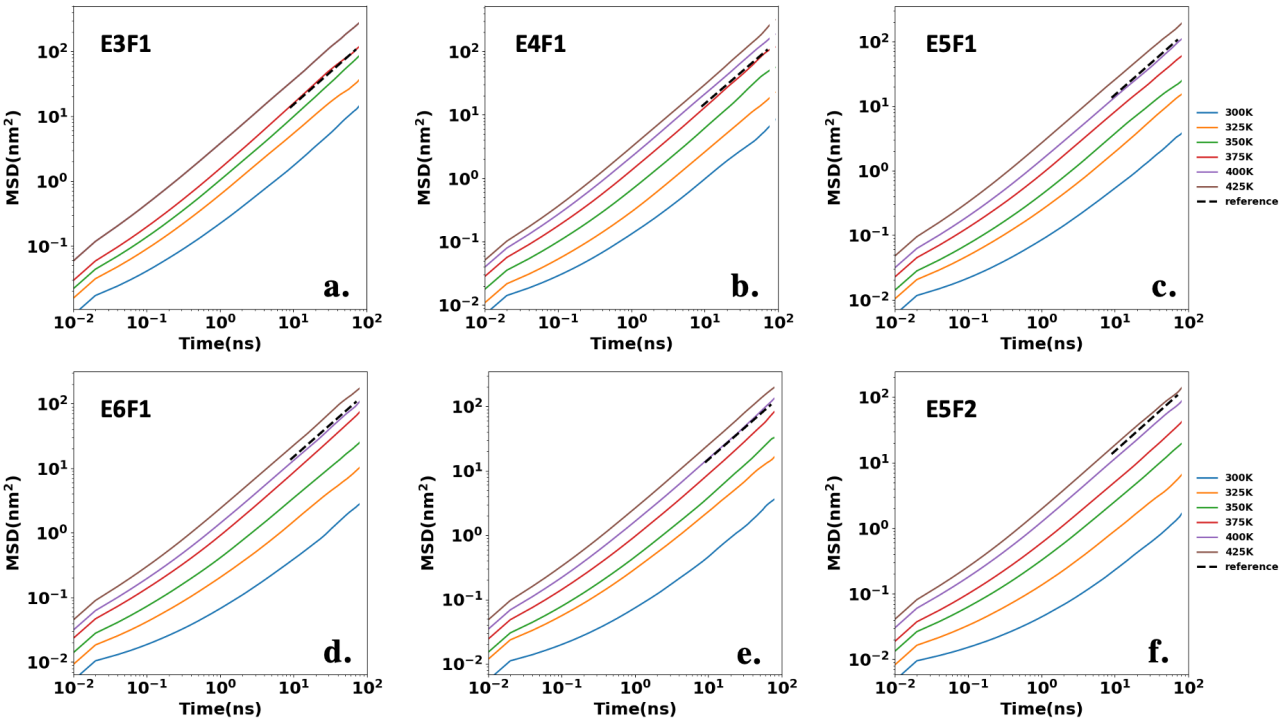

FIG. S.10. Li^+ ion MSD plots in (a) E3F1 (b) E4F1 (c) E5F1 (d) E6F1 (e) E3F2 (f) E5F2 at different temperatures in a log-log scale. The reference line with a unity slope is shown in black dashed line.

[1] S. Mogurampelly and V. Ganesan, The Journal of chemical physics **146**, 074902 (2017).

[2] D. J. Brooks, B. V. Merinov, W. A. Goddard III, B. Kozinsky, and J. Mailoa, Macromolecules **51**, 8987 (2018).

[3] N. Molinari, J. P. Mailoa, and B. Kozinsky, Chemistry of Materials **30**, 6298 (2018).

[4] W. L. Jorgensen, D. S. Maxwell, and J. Tirado-Rives, Journal of the American Chemical Society **118**, 11225 (1996).

[5] E. K. Watkins and W. L. Jorgensen, The Journal of Physical Chemistry A **105**, 4118 (2001).

[6] F. Neese, F. Wennmohs, U. Becker, and C. Riplinger, The Journal of chemical physics **152**, 224108 (2020).

[7] A. D. Becke, The Journal of chemical physics **104**, 1040 (1996).

[8] A. Simperler, A. Kornherr, R. Chopra, P. A. Bonnet, W. Jones, W. S. Motherwell, and G. Zifferer, The Journal of Physical Chemistry B **110**, 19678 (2006).

[9] J. Habasaki and K. Ngai, The Journal of chemical physics **129**, 194501 (2008).

[10] M. S. Kelkar and E. J. Maginn, The Journal of Physical Chemistry B **111**, 4867 (2007).